

FILTERS, COLOR CORRECTION AND CALIBRATION UNCERTAINTIES OF COMMON INSTRUMENTS

Frédéric GALLIANO

February 17, 2015

Contents

1	GENERAL FORMULAE FOR SYNTHETIC PHOTOMETRY	2
1.1	Photomultipliers	2
1.2	Bolometers	2
1.3	The Synthetic Photometry Subroutine	2
2	GENERAL COVARIANCE MATRIX FOR CALIBRATION UNCERTAINTIES	3
3	2MASS	6
3.1	Filters and Color Correction	6
3.2	Calibration errors	6
4	Akari IRC	6
4.1	Filters and Color Correction	6
4.2	Calibration errors	7
5	Spitzer IRAC	7
5.1	Filters and Color Correction	7
5.2	Calibration errors	8
6	WISE	8
6.1	Filters and Color Correction	8
6.2	Calibration errors	10
7	Akari FIS	10
7.1	Filters and Color Correction	10
7.2	Calibration errors	10
8	IRAS	10
8.1	Filters and Color Correction	10
8.2	Calibration errors	13
9	Spitzer MIPS	13
9.1	Filters and Color Correction	13
9.2	Calibration errors	14
10	Herschel PACS	14
10.1	Filters and Color Correction	14
10.2	Calibration errors	15
11	Herschel SPIRE	15
11.1	Filters and Color Correction	15
11.2	Calibration errors	16
12	Planck HFI	16
12.1	Filters and Color Correction	16
12.2	Calibration errors	16

1 GENERAL FORMULAE FOR SYNTHETIC PHOTOMETRY

1.1 Photomultipliers

A photomultiplier (like IRAC, MIPS, ISOCAM, etc.), counts the number of photons received by the detector, whatever their energy is. The spectral shape of the SED is important to derive the proper integrated flux within the band, in order to perform reliable color correction or synthetic photometry.

The number of photons per unit time, per surface area and per bin of frequency, from an incident flux F_ν is:

$$\frac{dN_\gamma}{dt dA d\nu} = \frac{F_\nu}{h\nu}. \quad (1)$$

If we note $R(\nu)$, the quantum efficiency of the filter in electrons per photons, then the rate of electrons per unit surface is:

$$\frac{dN_e}{dt dA} = \int \frac{F_\nu}{h\nu} R(\nu) d\nu. \quad (2)$$

Each instrument has a specific flux convention $F_\nu^{\text{conv.}}$, such that the flux in the band $F_{\nu_0}^{\text{band}}$ is the interpolated value of this specific SED at the nominal wavelength of the bandpass: $F_{\nu_0}^{\text{band}} = F_\nu^{\text{conv.}}(\nu_0)$. For a general SED, and any flux convention, the quoted flux in the band will be:

$$F_{\nu_0}^{\text{band}} = F_\nu^{\text{conv.}}(\nu_0) \times \frac{dN_e^{\text{actual}}}{dN_e^{\text{conv.}}} \quad (3)$$

$$= \frac{\int F_\nu R(\nu) \left(\frac{\nu_0}{\nu}\right) d\nu}{\int \left(\frac{F_\nu^{\text{conv.}}(\nu)}{F_\nu^{\text{conv.}}(\nu_0)}\right) R(\nu) \left(\frac{\nu_0}{\nu}\right) d\nu}. \quad (4)$$

If the convention is the common $F_\nu^{\text{conv.}} \propto \nu^{-\alpha}$, then the photometry is:

$$F_{\nu_0}^{\text{band}} = \frac{\int F_\nu R(\nu) \left(\frac{\nu_0}{\nu}\right) d\nu}{\int R(\nu) \left(\frac{\nu_0}{\nu}\right)^{\alpha+1} d\nu}. \quad (5)$$

1.2 Bolometers

A bolometer integrates the power received whatever the photon number count is. The power received per unit area, per unit frequency, is:

$$\frac{dE}{dt dA d\nu} = F_\nu. \quad (6)$$

If we note $R(\nu)$ the spectral response of the filter, the quoted flux in the band is then:

$$F_{\nu_0}^{\text{band}} = \frac{\int F_\nu R(\nu) d\nu}{\int \left(\frac{F_\nu^{\text{conv.}}(\nu)}{F_\nu^{\text{conv.}}(\nu_0)}\right) R(\nu) d\nu}. \quad (7)$$

1.3 The Synthetic Photometry Subroutine

The subroutine `synthetic_photometry` in the module `instrument_filters` performs synthetic photometry for all the filters listed in these notes. It builds an adaptative grid in wavelength in order to enforce a 10^{-3} accuracy on the derived quoted flux.

The accuracy of the comparison of the results of this subroutine to color correction tables given in observers' manuals is often more sensitive to the accuracy of the interpolation of the model (especially for very steep spectra), rather than to the actual accuracy of the integration. In any case, the systematic comparison shows that our routine is consistent with this table, most of the time, better than 1%.

2 GENERAL COVARIANCE MATRIX FOR CALIBRATION UNCERTAINTIES

In statistics, it is usual to decompose the covariance matrix as $\Sigma = S.R.S$, where S is the diagonal matrix whose elements are the standard deviations, and R is the correlation matrix. These matrices are given in Tables 1 and 2, for the calibration uncertainties of the instruments discussed in these notes.

Table 1: Standard-deviation matrix, S , in %.

[illegible]

[illegible]

3 2MASS

3.1 Filters and Color Correction

According to the [2MASS explanatory supplement](#), the filters provided are $\lambda R(\lambda)$, and are designed to be directly integrated over F_λ . Changing the SED to frequency dependence, we get:

$$F_{\nu_0}^{\text{band}} = \frac{\int F_\nu \left(\frac{\nu_0}{\nu}\right) R(\nu) d\nu}{\int \left(\frac{\nu_0}{\nu}\right)^3 R(\nu) d\nu}. \quad (8)$$

where $R(\nu)$ is the filter transmission (Fig. 1).

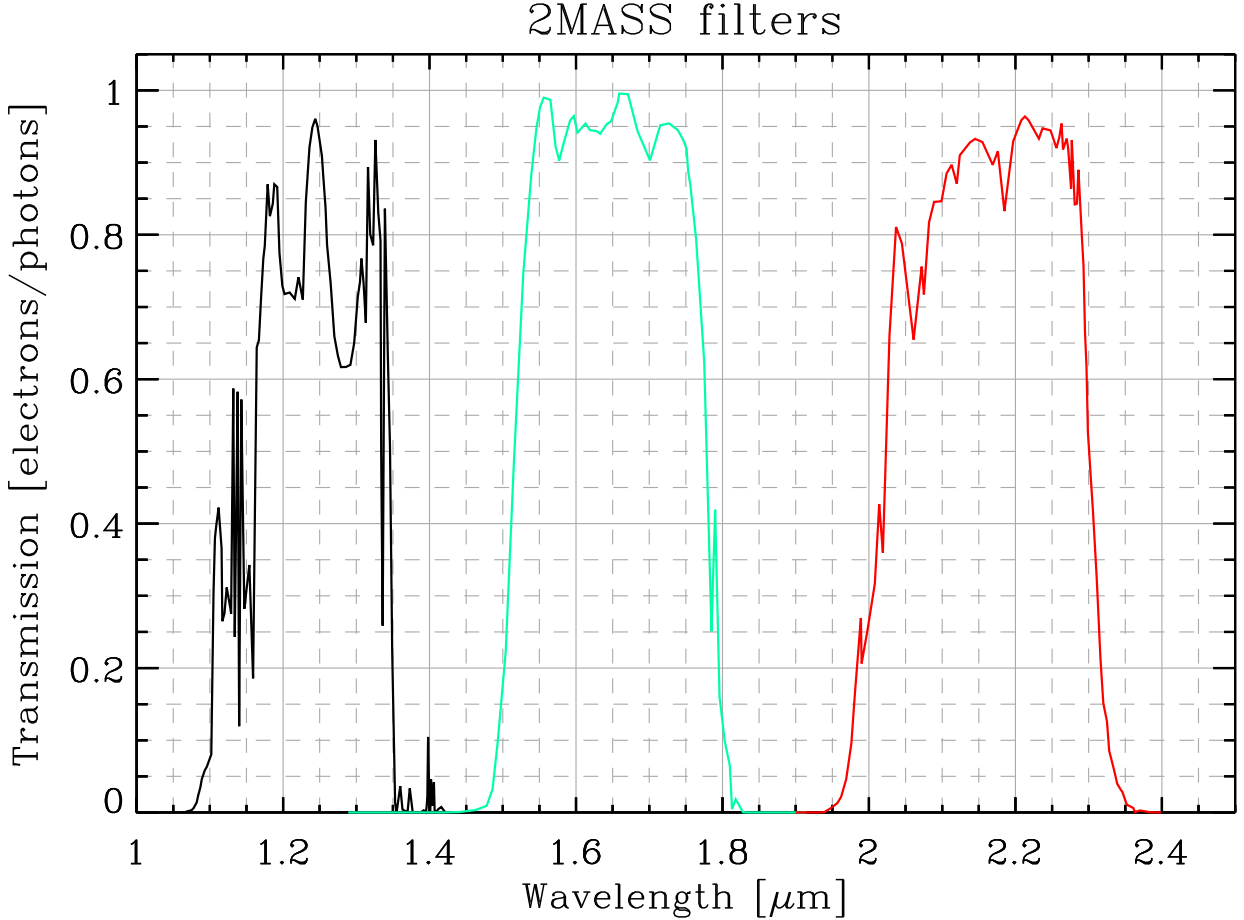


Figure 1: 2MASS filter transmission. Downloaded from [here](#). This is the quantum efficiency (QE).

I could not find a table of color corrections. Thus I could not check the accuracy of my routine, except by comparing it to S. Hony's code (agreement better than 3 %).

3.2 Calibration errors

The calibration is not clear. [Jarrett et al. \(2003\)](#) quotes a 2 – 3 % uncertainty on the zero-point magnitude. Since it is not clear, we assume a non-correlated 3 % calibration error, to be conservative.

4 Akari IRC

4.1 Filters and Color Correction

According Sect. 4.8 of the [Akari Data User Manual \(version 1.3\)](#), the flux quoted by the pipeline, F_ν^{band} , is related to the actual flux F_ν (the SED) and the transmission $R(\nu)$ (in electrons/photons; Fig. 2)

by:

$$F_{\nu_0}^{\text{band}} = \frac{\int \left(\frac{\nu_0}{\nu}\right) F_\nu R \, d\nu}{\int \left(\frac{\nu_0}{\nu}\right)^2 R \, d\nu}, \quad (9)$$

where ν_0 is the nominal frequency. We have tested this equation, using the filters downloaded from

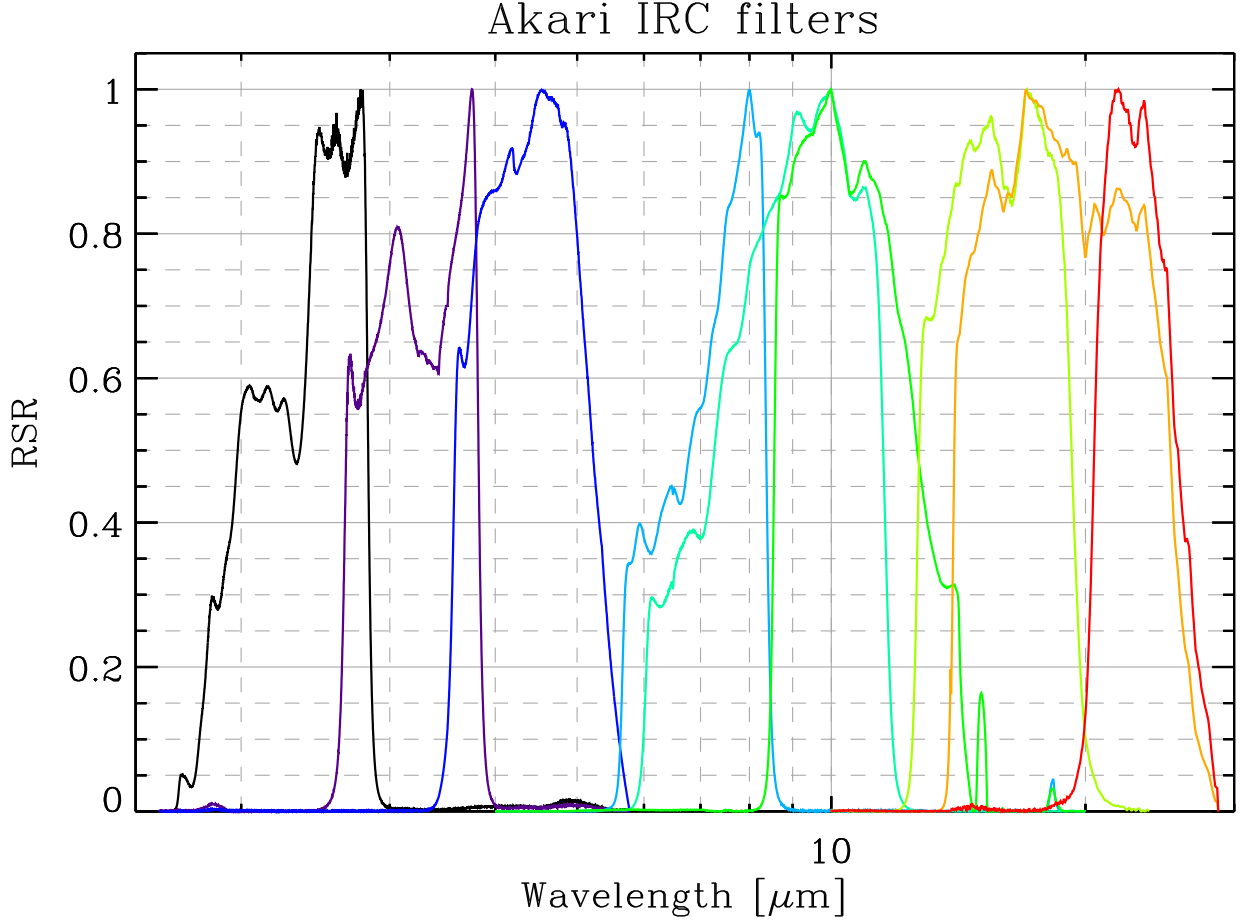


Figure 2: *Akari IRC transmission*. Downloaded from [here](#). This is the relative spectral response (the quantum efficiency divided by ν and scaled).

[here](#). These filters are actually $R_\nu(\nu) = R(\nu)/\nu$. Our routine is in agreement with Tables 4.8.8 and 4.8.11 of the [Akari Data User Manual \(version 1.3\)](#), with an accuracy better than 1 %.

4.2 Calibration errors

Table 4.6.7 of the [Akari Data User Manual \(version 1.3\)](#) quotes calibration uncertainties of each band, for point sources, ranging between 2 and 6 %. The degree of correlation between these calibration uncertainties is not clear from reading the manual. The calibration uncertainty of extended sources is not quantified either.

5 Spitzer IRAC

5.1 Filters and Color Correction

According to the [IRAC Instrument Handbook \(version 2.0.3; Eq. 4.8\)](#), the flux quoted by the pipeline, F_ν^{band} , is related to the actual flux F_ν (the SED) and the transmission $R(\nu)$ (in electrons/photons; Fig. 3) by:

$$F_{\nu_0}^{\text{band}} = \frac{\int \left(\frac{\nu_0}{\nu}\right) F_\nu R \, d\nu}{\int \left(\frac{\nu_0}{\nu}\right)^2 R \, d\nu}, \quad (10)$$

where ν_0 is the nominal frequency. We have tested this equation, using the filters downloaded from

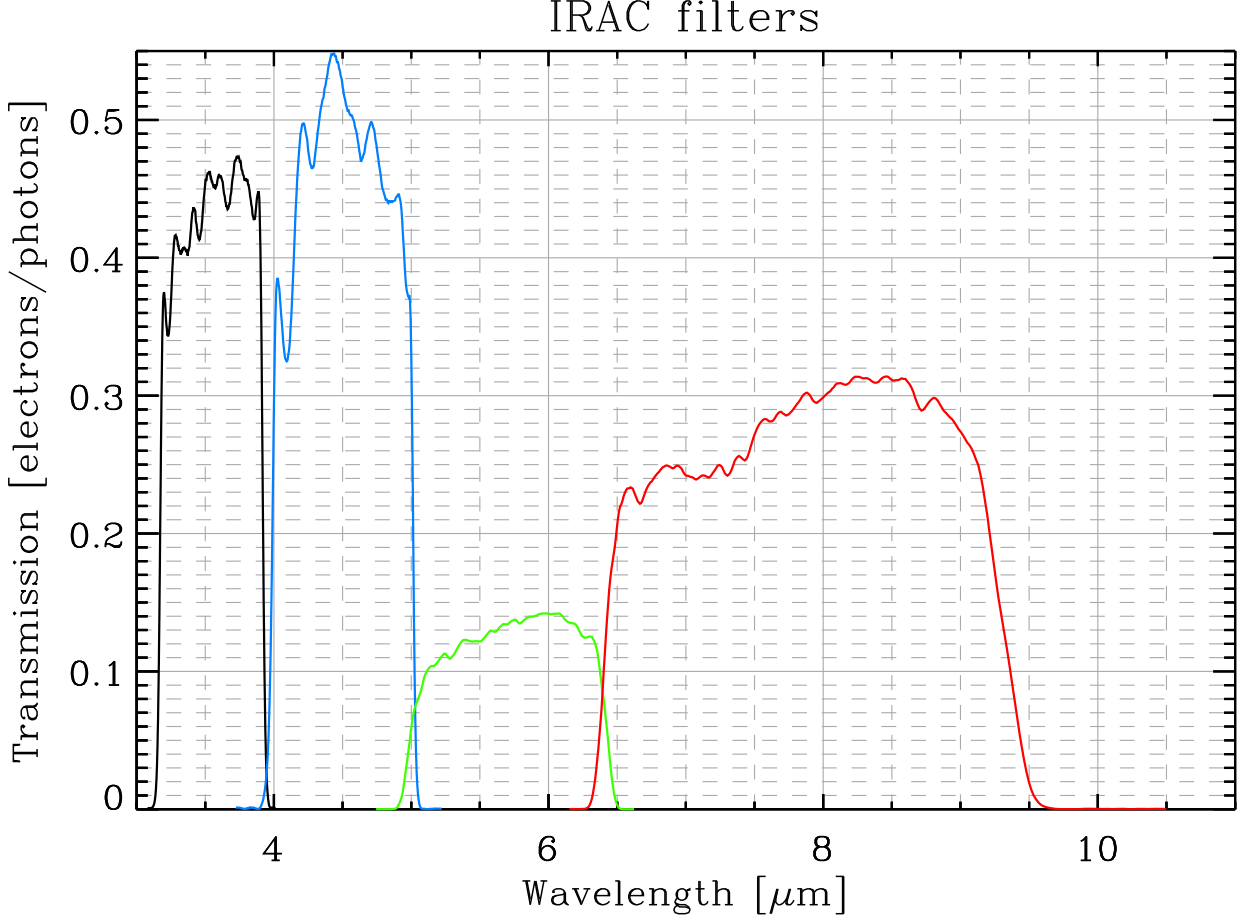


Figure 3: *IRAC transmission*. Downloaded from [here](#). This is the quantum efficiency (QE).

[here](#).

We have compared it to Tables 4.3 (power-law) and 4.4 (black body) of the [IRAC Instrument Handbook \(version 2.0.3\)](#), and the results are in agreement to better than 0.2 %.

5.2 Calibration errors

For extended sources, with a relatively flat surface brightness profile, the [IRAC Instrument Handbook \(version 2.0.3; Sect. 4.11.2\)](#) advises to apply aperture correction factors, for the infinite case of 0.91, 0.94, 0.73, 0.74 for $\text{IRAC}_{3.6\mu\text{m}}$, $\text{IRAC}_{4.5\mu\text{m}}$, $\text{IRAC}_{5.8\mu\text{m}}$, and $\text{IRAC}_{8\mu\text{m}}$ respectively. These apertures are accurate to 10 % (independent between wavelengths). This error should probably not be accounted as “systematic error”, as it depends on the actual morphology of the source, and therefore it is going to vary from one to place to another on a given image. Indeed, these aperture correction factors were derived from the surface brightness profile of elliptical galaxies.

[Reach et al. \(2005\)](#) quote a 2 % calibration error in all IRAC bands. According to Eq. (13) of [Reach et al. \(2005\)](#), it appears that σ_{abs} is the only correlated term error. Thus, the interband correlation coefficient is $\rho \simeq 0.29$.

6 WISE

6.1 Filters and Color Correction

According to the [online documentation](#), using the filters of Fig. 4, the color correction is:

$$F_{\nu_0}^{\text{band}} = \frac{\int \left(\frac{\nu_0}{\nu}\right) F_{\nu} R \, d\nu}{\int \left(\frac{\nu_0}{\nu}\right)^3 R \, d\nu}. \quad (11)$$

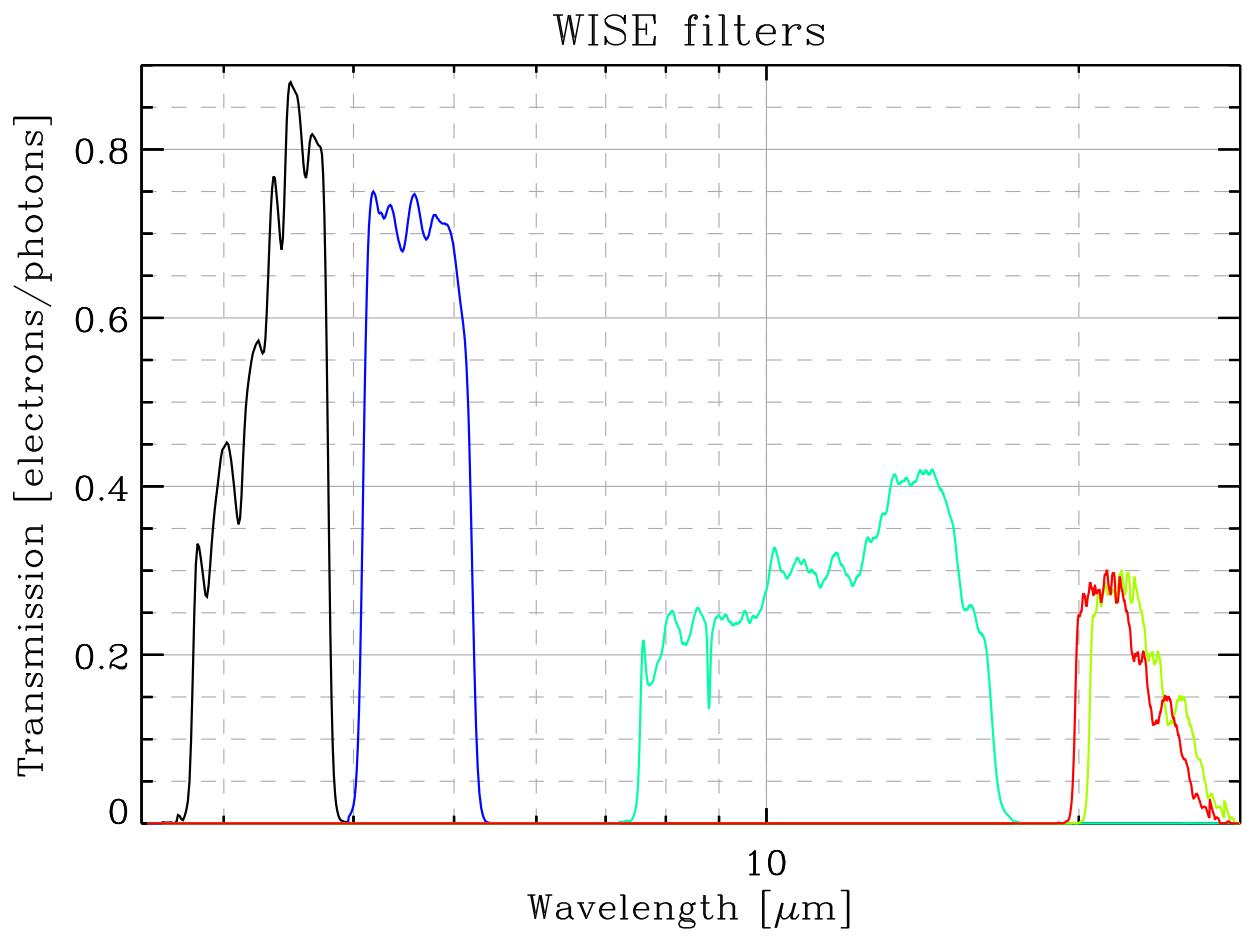


Figure 4: *WISE filter transmission*. Downloaded from [here](#). This is not the quantum efficiency (QE). To obtain the QE, one would have to divide these profiles by λ .

We have compared our routine to the results of [Wright et al. \(2010, or here\)](#), for power-law and black bodies. The results are in agreement, better than 0.2 %.

We also implement the revision of WISE4 by [Brown et al. \(2014\)](#), which simply consists in increasing the wavelength of the original RSRF by 3.3 %.

6.2 Calibration errors

The calibration of WISE is a mess. It is performed on observations of stars toward the Galactic pole, and tied to IRAC, MIPS, IRS and MSX by [Jarrett et al. \(2011\)](#). The rms part of the calibration error (independent between wavelengths; proper to WISE) is 2.4, 2.8, 4.5 and 5.7 %. To simplify, we can add and correlate the WISE1 and IRAC1 calibration errors, the WISE2 and IRAC2, the WISE3 and IRS-SL/LL and WISE4 and MIPS1. According to [Decin et al. \(2004\)](#), the IRS-LL calibration uncertainty is $\simeq 15$ %. In summary:

WISE1: $\sigma_{\text{cal}} = 3.2\%$ and $\rho_{\text{WISE1,IRAC1}} = 0.66$;

WISE2: $\sigma_{\text{cal}} = 3.5\%$ and $\rho_{\text{WISE2,IRAC2}} = 0.59$;

WISE3: $\sigma_{\text{cal}} = 15.7\%$ and $\rho_{\text{WISE3,IRS-LL}} = 0.96$.

WISE4: $\sigma_{\text{cal}} = 13.3\%$ and $\rho_{\text{WISE4,MIPS1}} = 0.30$.

7 Akari FIS

7.1 Filters and Color Correction

According to the [FIS DUM \(version 1.3\)](#), the color correction convention assumes a $\nu F_\nu = \text{const}$ spectrum:

$$F_{\nu_0}^{\text{band}} = \frac{\int \left(\frac{\nu_0}{\nu}\right) F_\nu R \, d\nu}{\int \left(\frac{\nu_0}{\nu}\right)^2 R \, d\nu}, \quad (12)$$

where $R(\nu)$ is the filter transmission (Fig. 5).

We have compared our routine to the color correction given in Table 4.2.2 of [FIS DUM \(version 1.3\)](#), and the agreements are better than 0.4 %.

7.2 Calibration errors

According to the [FIS DUM \(version 1.3\)](#), the calibration error is “*crudely*” estimated to be $\simeq 20\%$ in the SW band and $\simeq 30\%$ in the LW band. No correlation is specified.

8 IRAS

8.1 Filters and Color Correction

According to the [IRAS documentation](#), the color correction convention assumes a $\nu F_\nu = \text{const}$ spectrum:

$$F_{\nu_0}^{\text{band}} = \frac{\int \left(\frac{\nu_0}{\nu}\right) F_\nu R \, d\nu}{\int \left(\frac{\nu_0}{\nu}\right)^2 R \, d\nu}, \quad (13)$$

where $R(\nu)$ is the filter transmission (Fig. 6).

We have compared our routine to both power-laws and black bodies, given by the [IRAS online documentation](#). It is accurate better than 1 %, except for a power-law with $\alpha = 3$.

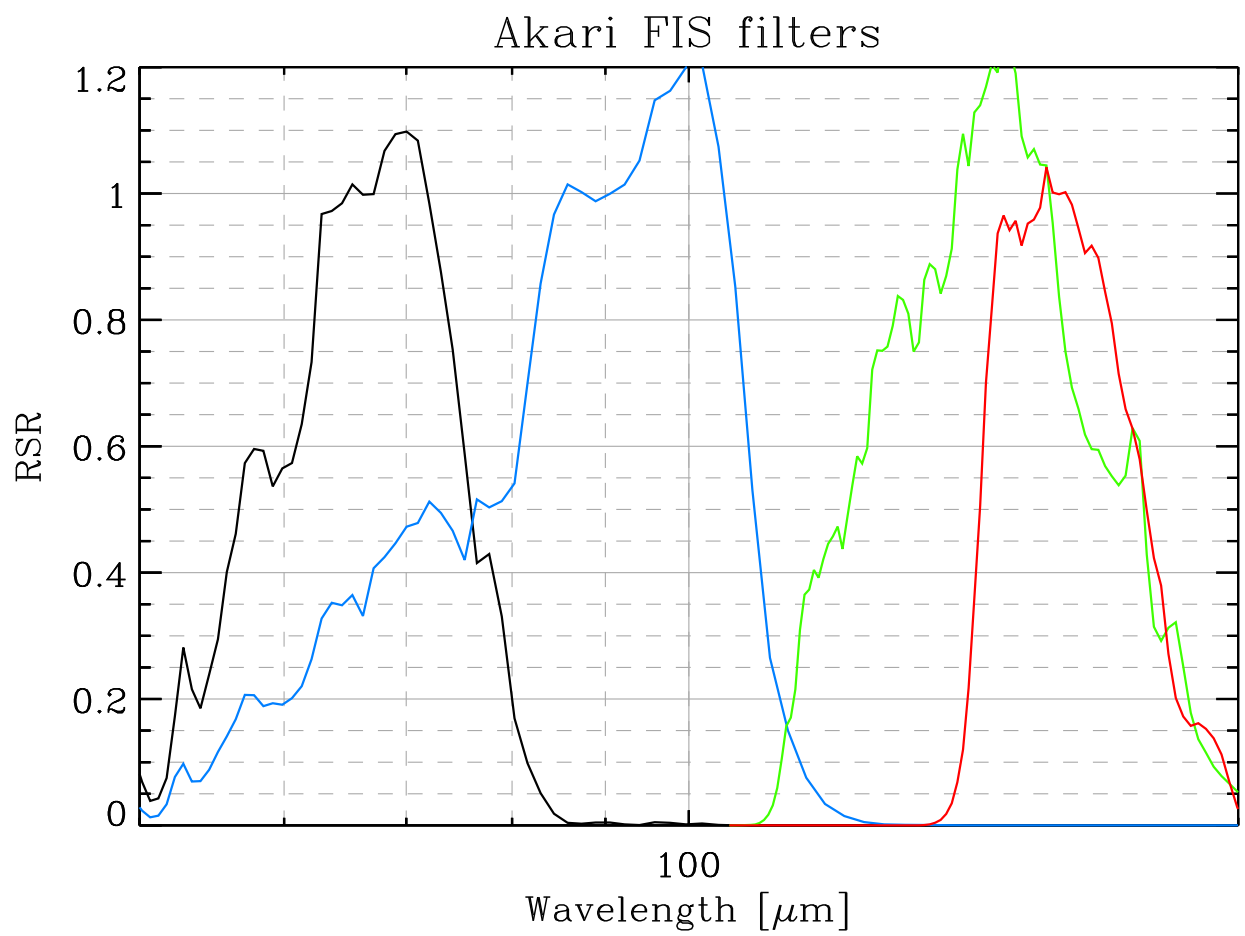


Figure 5: *FIS filter transmission*. Downloaded from [here](#). This is the relative spectral response (the quantum efficiency divided by ν and scaled).

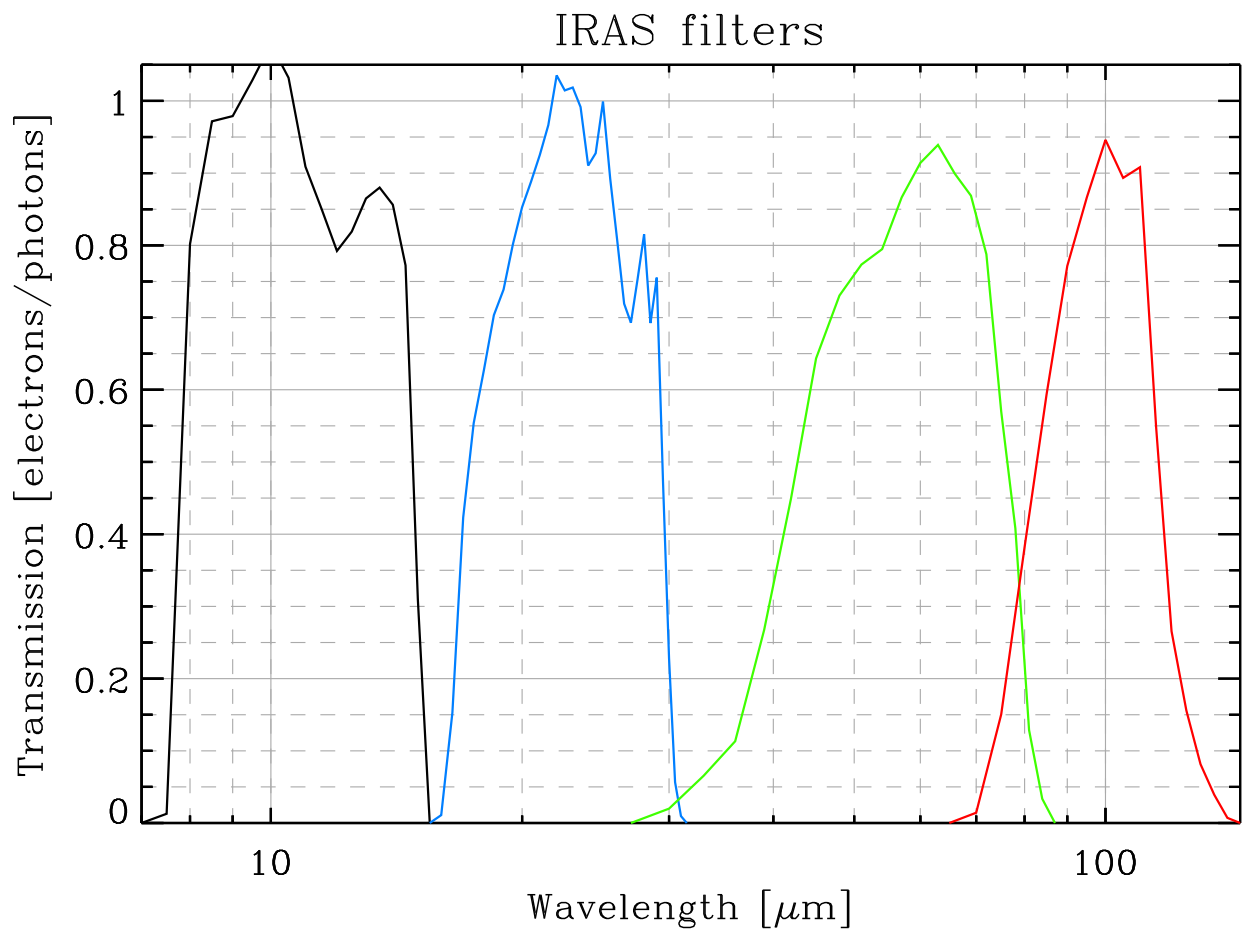


Figure 6: *IRAS filter transmission*. Downloaded from [here](#). This is the quantum efficiency (QE).

8.2 Calibration errors

According to the [IRAS explanatory supplement](#), the point source calibration of $\text{IRAS}_{12\mu\text{m}}$ is performed on α -Tau, the $\text{IRAS}_{25\mu\text{m}}$ and $\text{IRAS}_{60\mu\text{m}}$ extrapolation is made via models of stars. $\text{IRAS}_{60\mu\text{m}}$ and $\text{IRAS}_{100\mu\text{m}}$ are calibrated with asteroids. The uncertainties at 12, 25, and 60 μm , relative to the ground based 12 μm are 2, 5 and 5%. The absolute uncertainty on the 12 μm is 4%, common to the three bands. The correlation coefficients are therefore: $\rho_{\text{IRAS1,IRAS2}} = 0.56$, $\rho_{\text{IRAS1,IRAS3}} = 0.56$ and $\rho_{\text{IRAS2,IRAS3}} = 0.39$. The uncertainty at 100 μm is 10%.

The extended source calibration was based on the point source calibration. I could not find a document quantifying the additional errors due to the the fact that the source is extended.

9 Spitzer MIPS

9.1 Filters and Color Correction

According to the [MIPS Instrument Handbook \(version 3; Eq. 4.2\)](#), the flux quoted by the pipeline, F_{ν}^{band} , is related to the actual flux F_{ν} (the SED) and the transmission $R(\nu)$ (in electrons/photons; Fig. 7) by:

$$F_{\nu_0}^{\text{band}} = \frac{\int F_{\nu} R \, d\nu}{\int \frac{B_{\nu}(\nu, T_0)}{B_{\nu}(\nu_0, T_0)} R \, d\nu} \simeq \frac{\int F_{\nu} R \, d\nu}{\int \left(\frac{\nu}{\nu_0} \right)^2 R \, d\nu}, \quad (14)$$

with $T_0 = 10^4$ K. Note here that there is a λ factor missing in each integral compared to the Handbook. This is because the handbook requires to integrate over $R_{\lambda}(\lambda) = \lambda R(\lambda)$.

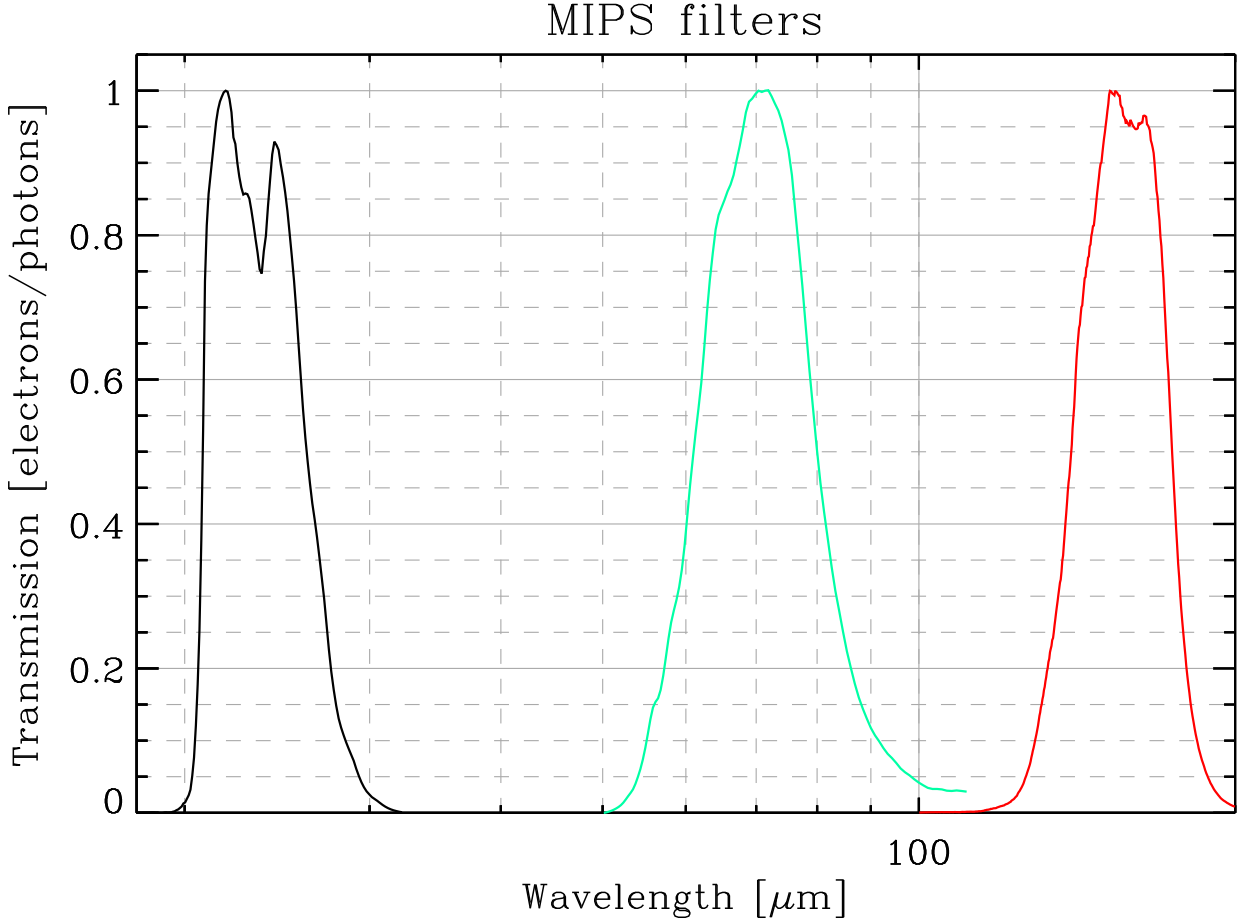


Figure 7: *MIPS transmission*. Downloaded from [here](#). This is the quantum efficiency (QE).

We have tested this equation, using the filters downloaded from [here](#). We have compared it to Tables 4.17 (power-law) and 4.16 (black body) of the [MIPS Instrument Handbook \(version 3\)](#), and the results are in agreement to better than 1%, for the whole range of parameters.

9.2 Calibration errors

The [MIPS Instrument Handbook \(version 3; Sect. 4.1.3\)](#) quotes a point source calibration error of 4 % for MIPS_{24μm} ([Engelbracht et al., 2007](#)), 5 % for MIPS_{70μm} ([Gordon et al., 2007](#)) and 12 % for MIPS_{160μm} ([Stansberry et al., 2007](#)). It also states that the calibration of extended sources is consistent with these values.

The samples used for calibration are different for each instrument. The primary calibrators are A stars for MIPS_{24μm}, B and M stars for MIPS_{70μm} and asteroids for MIPS_{160μm}. However, the calibration of MIPS_{160μm} is made using the MIPS_{24μm} and MIPS_{70μm} observations of asteroids. Therefore, we can consider that the calibration uncertainties of MIPS_{24μm} and MIPS_{70μm} are independent, but that they are correlated with MIPS_{160μm}. The correlation coefficients are: $\rho_{\text{MIPS1,MIPS3}} \simeq 0.33$, $\rho_{\text{MIPS2,MIPS3}} \simeq 0.42$.

10 Herschel PACS

10.1 Filters and Color Correction

The [ICC report \(May 2013\)](#) relates the PACS band flux to the SED (F_ν) by:

$$F_{\nu_0}^{\text{band}} = \frac{\int F_\nu R \, d\nu}{\int \left(\frac{\nu_0}{\nu}\right) R \, d\nu}, \quad (15)$$

where $R(\nu)$ is the filter transmission times the bolometer absorption.

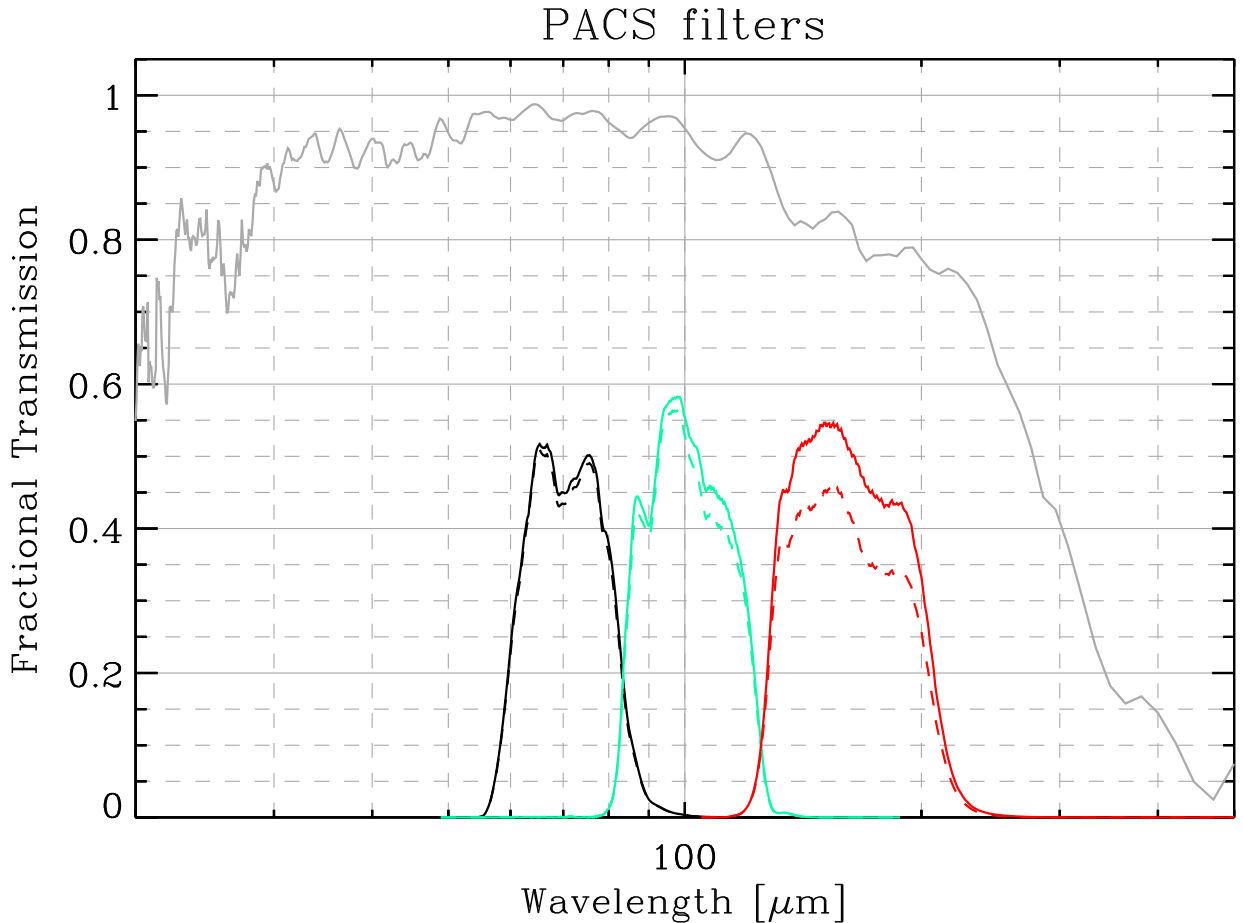


Figure 8: *PACS filter transmission* and bolometer absorption (in grey). Downloaded from [here](#). This is not the quantum efficiency (QE). To obtain the QE, one would have to divide these profiles by λ .

We have tested this equation, using the filters downloaded from [here](#) (Fig. 8). We have compared it to Tables 2 (black bodies) of the [ICC report \(May 2013\)](#), and the results are in agreement to better than 1 %.

10.2 Calibration errors

The calibration of PACS is performed on 5 fiducial stars (Müller *et al.* 2011; Sect. 6). The model uncertainty is about 5% and the RMS of the calibrator observations are 1.4%, 1.6% and 3.5% in PACS_{70μm}, PACS_{100μm} and PACS_{160μm}, respectively. The calibration errors, for point sources are therefore $\sigma_c = \sqrt{rms^2 + 0.05^2}/5$, which is 2.6%, 2.8% and 4.2%. There is correlation between the modelled fluxes. The correlation coefficients are $\rho_{IRAC1,IRAC2} = 0.69$, $\rho_{IRAC1,IRAC3} = 0.45$ and $\rho_{IRAC2,IRAC3} = 0.44$.

The calibration for extended sources, is likely higher than those. However, we could not find publications quantifying it exactly.

11 Herschel SPIRE

11.1 Filters and Color Correction

According to SPIRE observer's manual (version 2.4), the quoted flux in band for a point source is (same convention as PACS): relates the PACS band flux to the SED (F_ν) by:

$$F_{\nu_0}^{\text{band}} = \frac{\int F_\nu R \, d\nu}{\int \left(\frac{\nu_0}{\nu}\right) R \, d\nu}, \quad (16)$$

where $R(\nu)$ is the filter transmission, and for extended sources, the transmission is weighted by λ^2 :

$$F_{\nu_0}^{\text{band}} = \frac{\int \left(\frac{\nu_0}{\nu}\right)^2 F_\nu R \, d\nu}{\int \left(\frac{\nu_0}{\nu}\right)^3 R \, d\nu}. \quad (17)$$

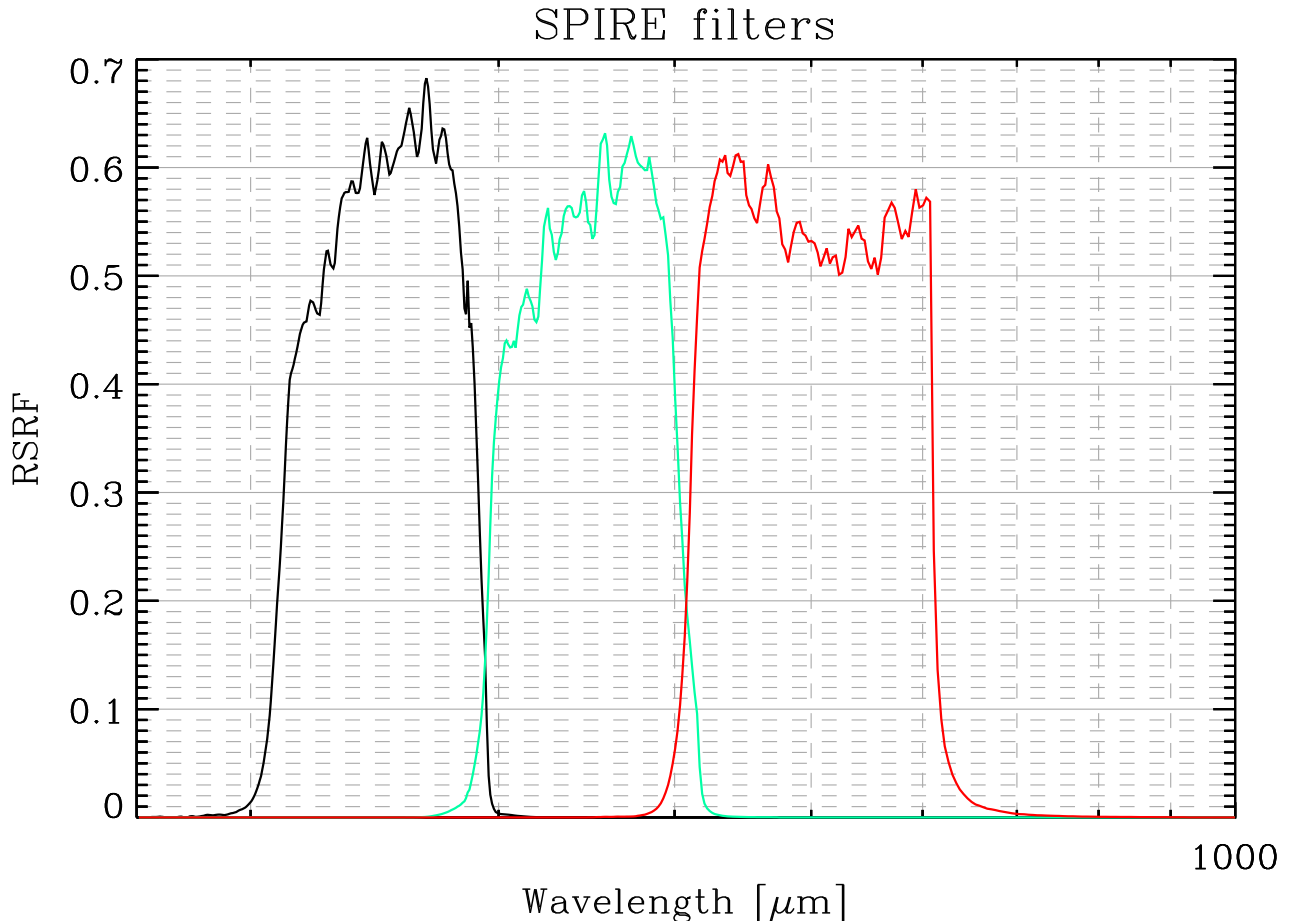


Figure 9: Point source SPIRE RSRFs. Downloaded from [here](#).

We have tested our routine on power-law spectra and compared to Table 5.3 of the [SPIRE observer’s manual \(version 2.4\)](#), for both point and extended sources, using the filters of Fig. 9. They are accurate better than 0.2 %.

11.2 Calibration errors

According to [SPIRE observer’s manual \(version 2.4; Sect. 5.2.8\)](#), if the data are *point source calibrated* only, the fluxes of extended sources must be multiplied by (0.9828, 0.9834, 0.9710).

The calibration errors, detailed by [Griffin et al. \(2013\)](#), are summarized on [SPIRE calibration page](#):

- 4 % due to the uncertainty on the Neptune model (correlated across the three bands);
- 1.5 % due to the noise of the observations of Neptune (independent);
- 4 % due to the beam area, for extended sources, only (independent).

Thus the calibration errors are 5.9 %, for each band, with the correlation coefficient $\rho = 0.47$.

12 Planck HFI

12.1 Filters and Color Correction

According to [Planck Collaboration et al. \(2013, Eq. 2\)](#), the quoted flux is related to the SED by:

$$F_{\nu_0}^{\text{band}} = \frac{\int F_{\nu} R(\nu) d\nu}{\int \left(\frac{\nu_0}{\nu}\right) R(\nu) d\nu}. \quad (18)$$

This is the synthetic photometry for a bolometer array, with the $\nu F_{\nu} = \text{const}$ convention.

We have compared our colour correction routine to the values given by the [UC CC software notes](#), for both power-laws and black bodies. The results are in agreement with an accuracy better than 1 %, except for the two short wavelength bands for a power-laws with indices $\alpha = -3, -4$, where the interpolation is steep.

12.2 Calibration errors

According to [Planck Collaboration et al. \(2013\)](#), the calibration of HFI is performed using Neptune and Uranus for the 545 and 857 GHz bands, and using the CMB dipole for the low frequencies. The various sources of uncertainties are summarized in Table 11 of [Planck Collaboration et al. \(2013\)](#). The last column (“*model*”) is the only one that induces a correlation between wavelengths.

References

- Brown, M. J. I., Jarrett, T. H., & Cluver, M. E. 2014, [ArXiv e-prints](#)
- Decin, L., Morris, P. W., Appleton, P. N., et al. 2004, [ApJS](#), **154**, 408
- Engelbracht, C. W., Blaylock, M., Su, K. Y. L., et al. 2007, [PASP](#), **119**, 994
- Gordon, K. D., Engelbracht, C. W., Fadda, D., et al. 2007, [PASP](#), **119**, 1019
- Griffin, M. J., North, C. E., Schulz, B., et al. 2013, [MNRAS](#), **434**, 992
- Jarrett, T. H., Chester, T., Cutri, R., Schneider, S. E., & Huchra, J. P. 2003, [AJ](#), **125**, 525
- Jarrett, T. H., Cohen, M., Masci, F., et al. 2011, [ApJ](#), **735**, 112
- Planck Collaboration, Ade, P. A. R., Aghanim, N., et al. 2013, [ArXiv e-prints](#)
- Reach, W. T., Megeath, S. T., Cohen, M., et al. 2005, [PASP](#), **117**, 978
- Stansberry, J. A., Gordon, K. D., Bhattacharya, B., et al. 2007, [PASP](#), **119**, 1038
- Wright, E. L., Eisenhardt, P. R. M., Mainzer, A. K., et al. 2010, [AJ](#), **140**, 1868

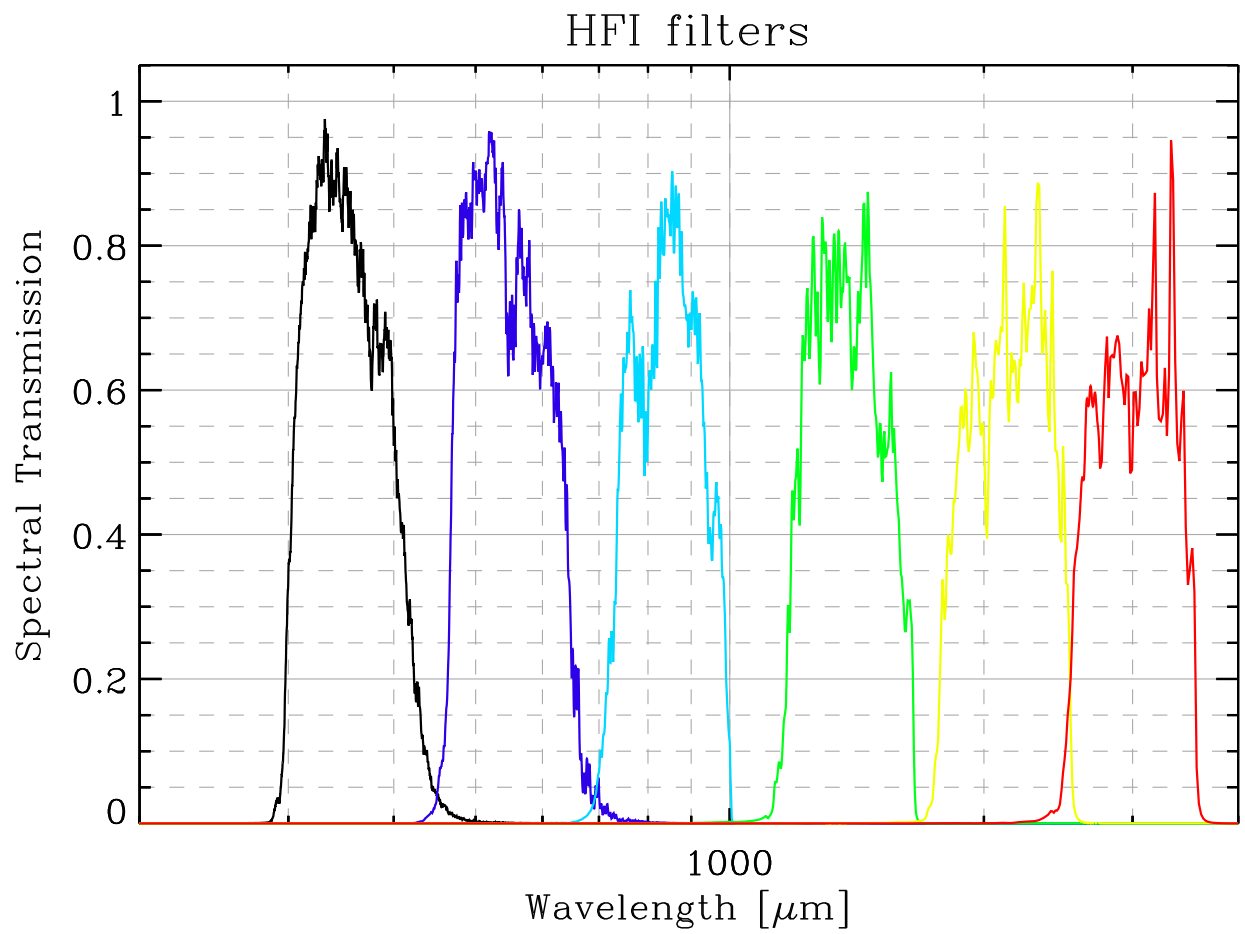


Figure 10: *HFI filter transmission*. Downloaded from [here](#). This is not the quantum efficiency (QE), since HFI is a bolometer array.